



1 Does drought advance the onset of  
2 autumn leaf senescence in temperate  
3 deciduous forest trees?  
4  
5

6 Bertold Mariën<sup>1,\*</sup>, Inge Dox<sup>1</sup>, Hans J De Boeck<sup>1</sup>, Patrick Willems<sup>2</sup>, Sebastien Leys<sup>1</sup>, Dimitri Papadimitriou<sup>3</sup> and Matteo  
7 Campioli<sup>1</sup>

8 <sup>1</sup>PLECO (Plants and Ecosystems), Department of Biology, University of Antwerp, 2160 Wilrijk, Belgium

9 <sup>2</sup>Hydraulics Division, KU Leuven, Kasteelpark Arenberg 40, 3001, Leuven, Belgium

10 <sup>3</sup>IDLab (Internet Data Lab), Department of Mathematics and Computer Science, University of Antwerp, 2000 Antwerp, Belgium

11  
12

13

14 \*Author for correspondence:

15 *Bertold Mariën*

16 *Tel: 032659333*

17 *Email: [bertold.marien@uantwerpen.be](mailto:bertold.marien@uantwerpen.be)*

18

19



20 **Abstract**

- 21 • Severe droughts are expected to become more frequent and persistent. However, their effect on  
22 autumn leaf senescence, a key process for deciduous trees and ecosystem functioning, is currently  
23 unclear. We hypothesized that (I) severe drought advances the onset of autumn leaf senescence  
24 in temperate deciduous trees and that (II) tree species show different dynamics of autumn leaf  
25 senescence under drought.
- 26 • We tested these hypotheses using a manipulative experiment on beech saplings and three years  
27 of monitoring mature beech, birch and oak trees in Belgium. The autumn leaf senescence was  
28 derived from the seasonal pattern of the chlorophyll content index and the loss of canopy  
29 greenness using generalized additive models and piece-wise linear regressions.
- 30 • Drought did not affect the onset of autumn leaf senescence in both saplings and mature trees,  
31 even if the saplings showed a high mortality and the mature trees a high leaf mortality (due to  
32 accelerated leaf senescence and early leaf abscission). We did not observe major differences  
33 among species.
- 34 • Synthesis: The timing of autumn leaf senescence appears conservative across years and species,  
35 and even independent on drought stress. Therefore, to study autumn senescence, seasonal  
36 chlorophyll dynamics and loss of canopy greenness should be considered separately.

62 **Key words**

63 Autumn leaf senescence, *Betula pendula*, Drought, *Fagus sylvatica*, Generalized additive mixed  
64 models, Leaf coloration and fall, *Quercus robur*, Rainfall deficit



## 65 1. Introduction

66 Autumn leaf senescence is a developmental stage of the leaf cells. The core function of this process is the  
67 remobilization of nutrients and death is its consequence (Medawar, 1957;Keskitalo et al., 2005). Its  
68 evolutionary purpose is likely stress resistance and, as such, the process dynamics are affected by different  
69 forms of environmental stress (e.g. high temperatures, water logging) (Benbella and Paulsen, 1998;Leul  
70 and Zhou, 1998;Munné-Bosch and Alegre, 2004). The process of autumn leaf senescence is highly  
71 coordinated and characterized by a tight control over its timing. Furthermore, its most manifest feature,  
72 the detoxification of chlorophyll, allows the degradation of leaf macromolecules and subsequent nutrient  
73 remobilization -the essence of autumn leaf senescence- (Hörtensteiner and Feller, 2002;Munné-Bosch  
74 and Alegre, 2004;Matile, 2000). In addition, chlorophyll degradation allows for the typical leaf coloration  
75 during autumn. However, autumn leaf senescence is also an important process at the ecosystem scale  
76 because it affects multiple ecological processes, such as trophic dynamics, tree growth or the exchange  
77 of matter and energy between the ecosystem and atmosphere (Richardson et al., 2013).

78  
79 Despite its relevance, literature on autumn senescence has maintained a wide variety of definitions and  
80 observational methods (Gill et al., 2015;Fracheboud et al., 2009;Gallinat et al., 2015). This has hampered  
81 our understanding of the effects of drought stress on the timing of the onset of autumn leaf senescence,  
82 as opposed to the timing of leaf abscission or accelerated leaf senescence. For example, Estiarte and  
83 Penuelas (2015) reported that leaf senescence advances due to drought stress, while Vander Mijnsbrugge  
84 et al. (2016) reported a delay in the leaf senescence of young trees subjected to drought. After the  
85 summer drought in central Europe of 2003, Leuzinger et al. (2005) even reported that the leaf longevity  
86 (measured as a delay in the leaf discoloration and fall) of five deciduous tree species was on average  
87 prolonged by 22 days.

88  
89 Droughts are expected to occur more frequently and become more intensive due to global warming and  
90 changes in precipitation patterns (IPCC, 2014;Crabbe et al., 2016). Extended periods with lower than  
91 average rainfall are often associated with higher air temperatures and higher vapor pressure deficits,  
92 which can negatively affect the functioning of trees in the temperate zone (Novick et al., 2016;De Boeck  
93 and Verbeeck, 2011). Belgian forests are thought to be especially vulnerable to droughts as they typically  
94 have sandy soils with low soil field capacities (Vander Mijnsbrugge et al., 2016;van der Werf et al., 2007).

95  
96 To examine the effects of drought stress on the onset of autumn leaf senescence, we hypothesized that:

- 97 (I) the timing of the onset of autumn leaf senescence in temperate deciduous trees is advanced  
98 by severe drought stress. The leaves of a tree that experiences a drought will accumulate the  
99 consequences of stress exposure and lose functionality. Therefore, it is likely not beneficial  
100 for a tree to maintain active leaves late in the season after a severe drought. Instead, to  
101 maximize nutrient recovery, trees probably prefer an earlier leaf senescence. In addition, a  
102 drought would reduce the tree's wood growth and increase its fine root mortality (Brunner  
103 et al., 2015;Campioli et al., 2013). Consequently, the tree's carbon sink strength will decline,  
104 causing a reduced demand for carbon from the sources (e.g. the leaves) and advance the  
105 onset of autumn leaf senescence.
- 106 (II) different tree species show different dynamics in their onset of autumn leaf senescence under  
107 drought. We hypothesized that, under drought stress, species with continuous flushing (e.g.  
108 birch) will have a more stable timing onset of autumn leaf senescence than species with only  
109 one or two leaf flushes during spring-summer (e.g. beech and oak) (Koike, 1990).

110



111 We tested these hypotheses by subjecting young trees to drought stress in an experimental set-up and by  
112 examining the effect of years with different drought intensities (2017, 2018 and 2019) on mature trees in  
113 natural forest stands.

## 114 2. Materials and methods

### 115 2.1. Study sites and experimental setting

#### 116 2.1.1. Manipulative drought experiment

117 In 2018, we carried out a manipulative drought experiment at the Drie Eiken Campus in Wilrijk, Belgium  
118 (51°09'N, 4°24'E). In early March, 128 individuals of three-year-old beech (*Fagus sylvatica*) saplings, from  
119 a local nursery and with the same local provenance, were planted in pots with a volume of 35 liters and a  
120 surface area of 0.07 m<sup>2</sup>. The pots were filled with 20% peat and 80% white sand. Eight beech saplings  
121 were placed in each of twelve climate-controlled glasshouses with a ground surface of 1.5 x 1.5 m and a  
122 height at the north and south side of 1.5 m and 1.2 m, respectively. The glasshouses had a roof of colorless  
123 polycarbonate (a 4 mm thick plate) reducing the incoming light by ± 20%, had three sides that could be  
124 opened or closed and were equipped with a combined humidity-temperature sensor (QFA66, Siemens,  
125 Erlangen, Germany) to monitor the relative humidity and air temperature (Fig. 1, panel A and B). One pot  
126 per glasshouse was also equipped with a soil moisture smart sensor (HOBO S-SMD-M005, Onset, MA,  
127 USA) to monitor the soil water content (Fig. 1, panel C). The latter sensors became available only at the  
128 time the drought stress was alleviated (see below). More details on the set-up of the glasshouses can be  
129 found in the literature (Van den Berge et al., 2011; De Boeck et al., 2012; Fu et al., 2014). Two treatments  
130 were organized (n = 48 per treatment; see below). In addition to the saplings in the glasshouses, eight  
131 beech saplings were placed in each of four reference plots outside of the glasshouses (n = 32, Ref.). The  
132 relative humidity and air temperature of the outside reference plots were monitored by a pocket weather  
133 meter (Kestrel 3000, Nielsen, PA, USA). Once in April and once in July, all saplings received 35 g of NPK  
134 slow-release fertilizer (DCM ECO-XTRA 1) and 1.8 g of micro elements (DCM MICRO-MIX). Using the  
135 relative humidity and air temperature data between 7 a.m. and 7 p.m., the vapor pressure deficit was  
136 calculated for both treatments (see below) and the reference plots using the formulas of Buck (1981) (Eq.  
137 1; Fig. 1, panel D).

138

139 Equation 1

140

$$e_0 = 613.75 \times \exp((17.502 \times T)/(240.97 + T))$$

141

$$e = RH \times e_0$$

142

$$VPD = e_0 - e$$

143

144 where  $e_0$  is the saturation vapor pressure (in kPa),  $T$  is the temperature (in °C),  $e$  is the actual vapor  
145 pressure deficit (in kPa),  $RH$  is the relative humidity (in %) and  $VPD$  is the vapor pressure deficit (in kPa).

146

147 From planting until April, the saplings were all irrigated two to three times a week until the pots  
148 overflowed. At the start of the treatment, in early May, we shielded all the glasshouses using polyethylene  
149 film (200 μm thick) and irrigated the saplings only once a week with circa 1.5 liter of water. In addition,  
150 we enhanced the drought in six glasshouses by raising the air temperature by three degrees compared to  
151 the ambient air temperature (+3 °C). The idea was to simulate 'natural' drought conditions, which are  
152 typically associated with warmer temperatures. The air temperature in the other six glasshouses followed  
153 the ambient air temperature (+0 °C). During the treatment, the daily soil water content and the daily  
154 relative humidity in the glasshouses with the +3 °C treatment were lower in comparison to the glasshouses  
155 with the +0 °C treatment. The difference was around 0.02 m<sup>3</sup>/m<sup>3</sup> for the soil water content and 20% for  
156 the relative humidity (Fig. 1). The plan was to continue the treatment till the end of June but, due to the  
157 significant mortality rate, we were obliged to alleviate the drought stress already from the 20<sup>th</sup> of June.



158 From July, the glasshouses were opened again and the saplings were irrigated four to five times a week  
159 until the end of the season. During the whole growing season, the reference plots outside were  
160 abundantly irrigated until the pots overflowed.

161  
162 A draw-back of the experiment is that the saplings in the reference plots received more incoming light  
163 (i.e.  $\pm 20\%$ ) than the saplings in the glasshouses (Van den Berge et al., 2011). However, as beech is a shade  
164 tolerant species, reduced light is unlikely to have limited the tree growth.

165

#### 166 *2.1.2. Field observations in deciduous forests*

167 From 2017 to 2019, we monitored the chlorophyll content index (CCI; a proxy for the chlorophyll  
168 concentration) and loss of canopy greenness of dominant mature trees in two forests near Antwerp; the  
169 Klein Schietveld in Kapellen (KS; 51°21'N, 4°37'E) and the Park of Brasschaat (PB; 51°12'N, 4°26'E). In the  
170 KS, we monitored the CCI of four beech trees and four birch (*Betula pendula*) trees. In the PB, we  
171 monitored the CCI of four beech trees and four oak (*Quercus robur*) trees. The loss of canopy greenness  
172 was observed for the same tree individuals and four additional tree individuals per species and site (thus  
173 for 32 trees in total). The two forests and their meteorological conditions are described in detail by Mariën  
174 et al. (2019), which also showed a lack of site effects on the autumn chlorophyll dynamics for the tree  
175 species studied here. To have a larger statistical sample, the data of the two beech stands (also of similar  
176 age and stem diameter) were aggregated.

177

178 For summer and autumn, we report here the average values for the temperature, precipitation, number  
179 of rainy days, relative humidity, sunshine duration and global solar radiation for the meteorological station  
180 of the Royal Meteorological Institute (KMI) in Ukkel, Belgium (Table 1). For these data, long-term averaged  
181 data was available. The temperature, relative humidity, vapor pressure deficit (see Eq. 1) and precipitation  
182 from 2017 to 2019 are presented in more detail using daily values that were measured at Brasschaat and,  
183 whenever necessary, gap-filled with data from the meteorological station in Woensdrecht, Netherlands  
184 (Fig. 2, panel A – B; panel D ). The meteorological data from Brasschaat was provided by the Flemish  
185 Institute for Nature and Forest (INBO) and the Integrated Carbon Observation System (ICOS), while the  
186 data from Woensdrecht was provided by the Royal Dutch Meteorological Institute (KNMI). The distance  
187 from Ukkel and Woensdrecht to sites is 60 km and 20 km, respectively. However, both locations show no  
188 major climatological differences with the KS and PB and are representative for the inter-annual variability  
189 experienced by the forests.

190

#### 191 *2.1.3. The rainfall deficit: an indicator of drought stress for 2017 - 2019*

192 To indicate the magnitude of the droughts, we computed the rainfall deficit from 2017 to 2019 using data  
193 on the relative humidity, solar radiation, wind speed, temperature and precipitation from the  
194 meteorological station in Ukkel. Here, the meteorological records go back the longest in Belgium. The  
195 rainfall deficit is computed on a daily basis by accumulating the daily potential evapotranspiration minus  
196 the daily amount of precipitation. This was done in two ways: (I) per hydrological year, starting from a  
197 zero deficit at the start of the hydrological year (1<sup>st</sup> of April) and (II) continuous computation, so no restart  
198 from 0 at the start of each hydrological year. The latter method has the benefit that the long-term effect  
199 of accumulated droughts from successive years is accounted for.

200

201 The potential evapotranspiration was computed by means of the method of Bultot et al. (1983), which is  
202 similar to the method of Penman (1948), but has parameters that are calibrated specifically for the local  
203 Belgian conditions. Unlike for the rainfall deficit starting from a zero deficit, we accounted in the  
204 calculation of the continuously computed rainfall deficit for the hydrological fraction in wet periods that



205 does not contribute to building up ground water reserves. At the station of Ukkel, daily precipitation and  
206 potential evapotranspiration data are available since more than 100 years. The precipitation data are  
207 collected since 1898 on the same location, and is measured using the same instrument. For this study, the  
208 data for the 100-year period 1901-2000 was considered as the reference period for the computation of  
209 long-term statistics on the rainfall deficit.

## 211 2.2. Measuring autumn leaf senescence: the chlorophyll content index and the loss of 212 canopy greenness

213 In the manipulative experiment from late-July until late-November, we measured the CCI of each tree  
214 sapling weekly by randomly selecting one leaf from the outer, middle and inner layer of the upper part of  
215 the crown. The CCI was measured using a chlorophyll content meter, which measures the optical  
216 absorbance in the 653 nm and 931 nm wavebands (CCM-200 plus, Opti-Sciences Inc., Hudson, NH, USA).  
217 Concurrently, we visually estimated the loss of canopy greenness (LOGG; scaled between 0 and 1) of each  
218 sapling following the method of Vitasse et al. (2011), which accounts for both the percentage of leaves  
219 that have changed color and the percentage of leaves that have fallen.

220  
221 For the 16 mature trees in the two forests and from the end of July to the end of November, tree-climbers  
222 collected leaves on eight occasions per year separated by two to three weeks. During each measurement  
223 day, they collected five sun-leaves and five shade-leaves from each tree. Afterwards, the CCI was  
224 immediately measured on the harvested leaves using the same chlorophyll content meter as described  
225 above. From early September to late November, the loss of canopy greenness was estimated in a similar  
226 fashion to the manipulative experiment for the 32 mature trees (Vitasse et al., 2011).

227  
228 Following the method of Mariën et al. (2019), we validated the CCI values by measuring also the  
229 chlorophyll concentrations (Fig. S1). In 2017 and 2018, on one occasion per month and using a 10-mm  
230 diameter cylinder, we collected samples of leaf tissue from the leaves of the mature trees for which we  
231 also measured the CCI. After storage at -80 °C, the samples were grounded using glass beads and a  
232 centrifuge. The result was dissolved in ethanol and the absorption of the solution was measured using a  
233 spectrophotometer (Smart Spec Plus Spectrophotometer, Bio-Rad) at different wavelengths for  
234 Chlorophyll a (662 nm) and chlorophyll b (644 nm). The chlorophyll concentrations could then be derived  
235 from the absorption values using the formulas described in Holm (1954) and Vonwettstein (1957).

## 237 2.3. Tree mortality in the manipulative experiment

238 In this study, we only considered those trees that defoliated due to autumn leaf senescence. Other tree  
239 saplings have died or defoliated completely due to accelerated leaf senescence during or just after the  
240 drought period. Since chlorophyll degradation is a common feature of both senescence processes and  
241 nutrient remobilization was only measured indirectly by CCI, we did not consider (I) tree saplings that  
242 showed an early or abrupt defoliation (without gradual coloration) before the 18<sup>th</sup> of August (n = 20) and  
243 (II) tree saplings with constant CCI values lower than three, the limit at which the values of the CCI meter  
244 can be interpreted, for the whole period from August to November (n = 18). Like in other studies, some  
245 defoliated tree saplings produced a few new leaves as last attempt to prevent death (Vander Mijnsbrugge  
246 et al., 2016;Turcsan et al., 2016). However, there were not enough of such leaves for meaningful analyses.

247



## 248 2.4. Statistical analyses

249 All statistical analyses were performed using R v.3.6.1. (R Core Team, 2020). The model assumptions were  
250 tested following Zuur et al. (2010) and using R/ggpubr (Kassambara, 2019). All graphical output is built  
251 using the packages R/GGPlot2, R/VIRIDIS and R/COWPLOT (Wickham, 2009;Wilke, 2019;Garnier, 2018).

### 253 2.4.1. Assessing the patterns of CCI and loss of canopy greenness using generalized additive 254 mixed models

255 The patterns of the CCI and loss of canopy greenness data from both our tree saplings and mature trees  
256 were assessed using generalized additive mixed models (GAMMs) built using the packages R/MGCV,  
257 R/GRATIA and R/DPLYR (Wood, 2011;Wickham et al., 2018;Simpson, 2020;Hastie and Tibshirani,  
258 1986;Pedersen et al., 2019). We used GAMMs because they allow more flexibility than other models (e.g.  
259 generalized linear models) to model the distribution parameter  $\mu$  (i.e. the mean of the observed random  
260 variable) and the continuous explanatory variables (Rigby and Stasinopoulos, 2005).

261  
262 To model the CCI of both our tree saplings and mature trees as a function of their covariates, Gaussian  
263 GAMMs with the identity link function were used (Table 2; Model Eq. 1, 3, 5, 7). To model the loss of  
264 canopy greenness of both our tree saplings and mature trees as a function of their covariates and because  
265 the loss of canopy greenness is scaled between 0 and 1, Binomial GAMMs with the logistic link function  
266 were used (Table 2; Model Eq. 2, 4, 6, 8). The GAMMs were chosen with the lowest AIC value (Akaike  
267 information criterion) and all factor-smooth interaction terms were smoothed using P-splines to address  
268 the large gap in data (i.e. from November to June) between the yearly sampling periods.

269  
270 For the CCI of the beech saplings, the fixed covariates were the *treatment* (categorical with three levels),  
271 *leaf place* (categorical with three levels) and *day of the year* (continuous; model 1). The interaction term  
272 was modelled as a factor-smooth interaction between the covariates *day of the year* and *treatment*. The  
273 dependency among observations of the same individual tree was incorporated by using *individual tree* as  
274 random intercept.

#### 275 Model 1

$$\begin{aligned} 276 & Y_{ij} \sim \text{Gaussian}(\mu_{ij}, \text{cst.}) \\ 277 & g(\mathbb{E}(Y_{ij})) = g(\mu_{ij}) \\ 278 & g(\mu_{ij}) = \text{Treatment}_{ij} + \text{Leaf\_place}_{ij} + f(\text{Doy}_{ij}, \text{Treatment}_{ij}) + \text{Individual\_tree}_i \end{aligned}$$

279  
280 where  $g$  is the identity link function,  $\mu_{ij}$  is the conditional mean,  $Y_{ij}$  is the  $j$ th observation of the response  
281 variable (i.e. the CCI) in Individual tree  $i$ , and  $i = 1, \dots, 128$ , and Individual tree $_i$  is the random intercept (Zuur  
282 et al., 2007;Zuur et al., 2016).

283 For the loss of canopy greenness of the beech saplings, the fixed covariates were the *treatment*  
284 (categorical with three levels) and *day of the year* (continuous; model 2). The interaction term and the  
285 dependency among observations of the same individual tree were treated as in model 1.

#### 286 Model 2

$$\begin{aligned} 287 & Y_{ij} \sim \text{B}(n_{ij}, \pi_{ij}) \\ 288 & g(\mathbb{E}(Y_{ij})) = g(\mu_{ij}) \\ 289 & g(\mu_{ij}) = \text{Treatment}_{ij} + f(\text{Doy}_{ij}, \text{Treatment}_{ij}) + \text{Individual\_tree}_i \end{aligned}$$

290  
291 where  $n_{ij}$  is the number of observations,  $\pi_{ij}$  is the probability of ‘success’,  $g$  is the logit link function,  $\mu_{ij}$  is  
292 the conditional mean,  $Y_{ij}$  is the  $j$ th observation of the response variable (i.e. the loss of canopy greenness)  
293 in Individual tree  $i$ , and  $i = 1, \dots, 128$ , and Individual tree $_i$  is the random intercept.



294 For the CCI of the mature beech, birch and oak trees, the fixed covariates were the *year* (categorical with  
295 three levels), *leaf type* (categorical with two levels) and *day of the year* (continuous; model 3). The  
296 interaction term was modelled as a factor-smooth interaction between the covariates *day of the*  
297 *year* and *year*. The dependency among observations of the same individual tree was incorporated  
298 using *individual tree* as random intercept.

299 Model 3

$$\begin{aligned} 300 & Y_{ij} \sim \text{Gaussian}(\mu_{ij}, \text{cst.}) \\ 301 & g(\mathbb{E}(Y_{ij})) = g(\mu_{ij}) \\ 302 & g(\mu_{ij}) = \text{Year}_{ij} + \text{Leaf\_type}_{ij} + f(\text{DoY}_{ij}, \text{Year}_{ij}) + \text{Individual\_tree}_i \end{aligned}$$

304 where  $g$  is the identity link function,  $\mu_{ij}$  is the conditional mean,  $Y_{ij}$  is the  $j$ th observation of the response  
305 variable (i.e. the CCI) in Individual tree  $i$ , and  $i = 1, \dots, 8$  for beech,  $i = 1, \dots, 4$  for birch and  $i = 1, \dots, 4$  for oak,  
306 and Individual tree $_i$  is the random intercept.

307 For the loss of canopy greenness of the mature beech, birch and oak trees, the fixed covariates were the  
308 *year* (categorical with three levels) and *day of the year* (continuous; model 4). The interaction term and  
309 the dependency among observations of the same individual tree were treated as in model 3.

310 Model 4

$$\begin{aligned} 311 & Y_{ij} \sim \text{B}(n_{ij}, \pi_{ij}) \\ 312 & g(\mathbb{E}(Y_{ij})) = g(\mu_{ij}) \\ 313 & g(\mu_{ij}) = \text{Year}_{ij} + f(\text{DoY}_{ij}, \text{Year}_{ij}) + \text{Individual\_tree}_i \end{aligned}$$

315 where  $n_{ij}$  is the number of observations,  $\pi_{ij}$  is the probability of ‘success’,  $g$  is the logit link function,  $\mu_{ij}$  is  
316 the conditional mean,  $Y_{ij}$  is the  $j$ th observation of the response variable (i.e. the loss of canopy greenness)  
317 in Individual tree  $i$ , and  $i = 1, \dots, 16$  for beech,  $i = 1, \dots, 8$  for birch and  $i = 1, \dots, 8$  for oak, and Individual  
318 tree $_i$  is the random intercept.

#### 319 2.4.2. Using breakpoints to indicate the onset of autumn leaf senescence and the loss of canopy 320 greenness

321 In principle, the onset of autumn leaf senescence could be derived from the CCI or loss of canopy  
322 greenness. However, Mariën et al. (2019) recently showed that the latter method cannot be used under  
323 severe drought stress. Therefore, two phenological variables were considered to describe the autumn  
324 canopy dynamics: the onset of autumn leaf senescence derived from the CCI (the onset of autumn leaf  
325 senescence<sub>CCI</sub>) and the onset of the loss of canopy greenness. For each tree, we defined the onset of  
326 autumn leaf senescence and the onset of loss of canopy greenness as the date by which the variable of  
327 interest started to decline substantially in early autumn. These dates were calculated using piecewise  
328 linear regressions and are represented by the breakpoints resulting from these analyses (Menzel et al.,  
329 2015; Mariën et al., 2019; Xie and Wilson, 2020). The piecewise linear regressions were performed using  
330 R/DPLYR and R/SEGMENTED (Vito and Muggeo, 2008). The uncertainty reported represents the inter-tree  
331 variability. Trees that did not show a clear breakpoint (13 in the manipulative experiment) were not  
332 considered in the analysis. These trees did not show a different pattern of CCI or loss of canopy greenness  
333 than the other trees (Fig. S2).

#### 335 2.4.3. Comparing the onset of autumn leaf senescence among tree saplings exposed to different 336 drought treatments

337 We tested whether the beech saplings exposed to the three treatments in 2018 differed in their onset of  
338 autumn leaf senescence<sub>CCI</sub> using a linear model with the onset of autumn leaf senescence<sub>CCI</sub> as response





339 variable and *treatment* (categorical with three levels) as fixed covariate. The residuals of the model were  
340 approximately normally distributed and a Breusch-Pagan test, the  $R/\text{ncvTest}$  and  $R/\text{bptest}$  in the  $R/\text{CAR}$  and  
341  $R/\text{LMTTEST}$  packages, showed no evidence of heteroscedasticity ( $P > 0.05$ ) (Fox and Weisberg, 2019; Zeileis  
342 and Hothorn, 2002). A one-way ANOVA was used to detect significant differences in the onset of autumn  
343 leaf senescence<sub>CCI</sub> among the treatments.  
344

#### 345 2.4.4. Comparing the onset of autumn leaf senescence and the onset of loss of canopy greenness 346 in mature trees among species and years

347 To model the onset of autumn leaf senescence<sub>CCI</sub> and the onset of the loss of canopy greenness as a  
348 function of their covariates, Gaussian linear mixed models were used. These models were built with the  
349 package  $R/\text{LME4}$  (Bates et al., 2015).  
350

351 The effect of the year on the onset of autumn leaf senescence<sub>CCI</sub> and the onset of the loss of canopy  
352 greenness was assessed using two linear mixed effect models with the onset of autumn leaf senescence<sub>CCI</sub>  
353 and the onset of the loss of canopy greenness from the mature beech, birch and oak trees as response  
354 variable. The fixed covariate in these two models was the *Year* (categorical with three levels; model 5). To  
355 incorporate the dependency among observations of the same species, we used *species* as random  
356 intercept.

#### 357 Model 5

$$\begin{aligned} 358 & Y_{ij} \sim \text{Gaussian}(\mu_{ij}, \text{cst.}) \\ 359 & g(\mathbb{E}(Y_{ij})) = g(\mu_{ij}) \\ 360 & \mu_{ij} = \text{Year}_i + \text{Species}_i \\ 361 & \end{aligned}$$

362 where  $g$  is the identity link function,  $\mu_{ij}$  is the conditional mean,  $Y_{ij}$  is the  $j$ th observation of the response  
363 variable in *Species*  $i$ , and  $i = 1, \dots, 3$  and  $\text{Species}_i$  is the random intercept.

364 The effect of the species on the onset of autumn leaf senescence<sub>CCI</sub> and the onset of the loss of canopy  
365 greenness was assessed using two linear mixed effect models with the onset of autumn leaf senescence<sub>CCI</sub>  
366 and the onset of the loss of canopy greenness from the mature beech, birch and oak trees as response  
367 variable. The fixed covariate in these two models was the *Species* (categorical with three levels; model 6).  
368 To incorporate the dependency among observations of the same year, we used *Year* as random intercept.

#### 369 Model 6

$$\begin{aligned} 370 & Y_{ij} \sim \text{Gaussian}(\mu_{ij}, \text{cst.}) \\ 371 & g(\mathbb{E}(Y_{ij})) = g(\mu_{ij}) \\ 372 & \mu_{ij} = \text{Species}_i + \text{Year}_i \\ 373 & \end{aligned}$$

374 where  $g$  is the identity link function,  $\mu_{ij}$  is the conditional mean,  $Y_{ij}$  is the  $j$ th observation of the response  
375 variable in *Year*  $i$ , and  $i = 1, \dots, 3$  and  $\text{Year}_i$  is the random intercept.

376 The residuals of the models were approximately normally distributed and showed no heteroscedasticity  
377 (tested using diagnostic plots). Therefore, we used Pearson's chi-square test,  $R/\text{drop1}$  in the  $R/\text{LME4}$   
378 package, to detect significant differences in the onset of autumn leaf senescence and the onset of the loss  
379 of canopy greenness among the predictor variables. A multiple comparison test, the  $R/\text{glht}$  test with  
380 method Tukey in the  $R/\text{MULTCOMP}$  package, was used to test for significant differences among the means  
381 of the levels in the predictor variables (Hothorn et al., 2008).



### 382 3. Results

#### 383 3.1. Magnitude of the drought stress in 2017, 2018 and 2019

384 The weather in 2018 and 2019 was exceptional, as can be seen in the overview of the meteorological  
385 conditions from 2017 to 2019 against the long-term reference values in Table 1 and Figure 2. In 2017, the  
386 weather during spring was dry and warm but the weather during summer and autumn was relatively  
387 normal (KMI, 2017c, b, a). In contrast, the warm and dry summer of 2018 was marked by abnormal (with  
388 an average return time of 6 years) to exceptional (with an average return time of 30 years or more) values  
389 (KMI, 2018a). Furthermore, the autumn of 2018 was abnormally dry and all precipitation fell on relatively  
390 few days (32) (KMI, 2018b). In the summer of 2019, the average air temperature and the total amount of  
391 sunshine were both among the three highest values recorded since 1981. In fact, the absolute maximum  
392 air temperature record for Belgium was broken in 2019 (KMI, 2019b). On the other hand, the autumn of  
393 2019 was considered normal (KMI, 2019a).

394  
395 The rainfall deficit for each day in the hydrological year (from the 1<sup>st</sup> of April until the 31<sup>st</sup> of March) and  
396 different return times are shown in Figure 3 (panel A & B). This demonstrates that in the late spring of  
397 2017, the summer of 2018 and the summer of 2019 the rainfall deficit reached a return time between 20  
398 and 50 years, 50 years, and 20 years, respectively. The hydrological summers of 2017, 2018 and 2019 had  
399 therefore moderate to extremely dry conditions, which led to accumulated rainfall deficit conditions over  
400 time (see Figure 3; panel A). Especially the hydrological year starting in 2018 ended with a strong rainfall  
401 deficit of about 150 mm, which was not reduced during 2019.

402

#### 403 3.2. The effect of drought on the onset of autumn leaf senescence in tree saplings in a 404 manipulative experiment

405 For all treatments, the CCI values of the beech saplings showed an overall moderate decrease until the  
406 beginning of October. Afterwards, this decrease accelerated (Fig. 4; panel A & C; Table 2). In the +0 and  
407 especially the +3 °C treatment, an abnormal CCI decline was observed in early August with only a partial  
408 recovery later on. As a result, from the beginning of August until mid-September, the CCI values of the  
409 beech saplings in the reference plots were significantly higher than the CCI values of the beech saplings in  
410 the glasshouses. However, no significant difference was detected in the timing of the onset of autumn  
411 leaf senescence<sub>CCI</sub> among the beech saplings exposed to the three different treatments, as the mean onset  
412 of autumn leaf senescence<sub>CCI</sub> was between the 21<sup>st</sup> (DOY = 260 ± 5) and 25<sup>th</sup> (DOY = 264 ± 4) of September  
413 ( $P = 0.7$ ; Fig. S3).

414

415 The ~~loss of~~ canopy greenness for the beech saplings showed a stable decline from early August until the  
416 end of autumn (Fig. 4; panel B & D; Table 2). Nevertheless, during September, the ~~loss of~~ canopy greenness  
417 of the beech saplings in the reference plots was significantly higher than the ~~loss of~~ canopy greenness of  
418 the beech saplings in the glasshouses with the +3 °C treatment.

419

420 The tree saplings in the glasshouses of both treatments were exposed to a high mortality with 14% and  
421 26% of the tree saplings in the glasshouses with the +0 °C and +3 °C treatment, respectively, considered  
422 'dead' along our criteria (see §2.3.). In the reference plots, no beech saplings died.

423



424 3.3. Inter-annual and inter-species variability in the timing of the onset of autumn leaf senescence  
425 and the onset of the loss of canopy greenness in mature trees

426 The pattern in the CCI values for the mature beech, birch and oak trees seems consistent throughout the  
427 years with stable values in summer and a rapid decline around late October (Fig. 5 - 7; panel A & C; Table  
428 2). We also observed no significant difference in the onset of autumn leaf senescence<sub>CCI</sub> among the years  
429 ( $P = 0.09$ ) and species ( $P = 1$ ). The mean onset of autumn leaf senescence<sub>CCI</sub> among the years was from  
430 the 8<sup>th</sup> (DOY =  $281 \pm 6$ ) to the 19<sup>th</sup> (DOY =  $292 \pm 6$ ) of October (Fig. S4; panel A), while the mean onset of  
431 autumn leaf senescence<sub>CCI</sub> among the species was around the 13<sup>th</sup> of October (DOY =  $286 \pm 6$ ; Fig. S4;  
432 panel B). The CCI correlated linearly with the chlorophyll concentrations but the data showed more  
433 variation in 2018 than 2017 (see Fig. S1).

434  
435 The pattern in the loss of canopy greenness for the mature beech, birch and oak trees seemed less  
436 consistent throughout the years (Fig. 5 - 7; panel B & D; Table 2). The loss of canopy greenness showed a  
437 very similar pattern between 2017 and 2019 for birch and beech, with the start of the decline in canopy  
438 greenness values around late September for birch and late October for beech. Like beech and birch, oak  
439 showed a standard pattern in 2019 with the start of the seasonal decline in late October. However, in  
440 2017, oak showed an earlier loss of canopy greenness with the start of the seasonal decline in mid-  
441 September. In all cases, a rapid decline in the canopy greenness was observed in late autumn. In 2018, all  
442 species showed an earlier and steeper decline in their canopy greenness values. This effect was also  
443 reflected by a significant difference in the onset of the loss of canopy greenness among the years ( $P = 5 \times$   
444  $10^{-11}$ ). Across species, the onset of the loss of canopy greenness did not differ significantly ( $P = 0.9$ )  
445 between 2017 (DOY =  $292 \pm 9$ ) and 2019 (DOY =  $290 \pm 4$ ), while it occurred 26 and 25 days earlier in 2018  
446 (DOY =  $266 \pm 4$ ) compared to 2017 ( $P = 1 \times 10^{-5}$ ) and 2019 ( $P = 1 \times 10^{-5}$ ), respectively (Fig. S5; panel A).  
447 However, all tree species differed significantly in their onset of the loss of canopy greenness across years  
448 ( $P = 6 \times 10^{-9}$ ). Compared to birch (DOY =  $268 \pm 9$ ; Fig. S5; panel B), the onset of the loss of canopy greenness  
449 for beech was on average 16 days later ( $P = 1 \times 10^{-4}$ ; DOY =  $284 \pm 4$ ), while for oak this was 30 days later  
450 ( $P = 1 \times 10^{-4}$ ; DOY =  $298 \pm 4$ ). The onset of the loss of canopy greenness for beech was also 14 days earlier  
451 than that for oak ( $P = 7 \times 10^{-4}$ ).

452 4. Discussion

453 Our results showed that the timing of the onset of autumn leaf senescence in both tree saplings and  
454 mature trees was not significantly altered by severe drought stress induced by a decline in the soil  
455 moisture, relative humidity, and an increase in the air temperature and vapor pressure deficit. These  
456 results are in contrast to other studies reporting, for example, that drought stress delays the onset of  
457 autumn leaf senescence (determined using remote sensing indices or visual assessment) (Wang et al.,  
458 2016; Vander Mijnsbrugge et al., 2016; Zeng et al., 2011; Gárate-Escamilla et al., 2020; Seyednasrollah et al.,  
459 2020). However, in our study, drought stress did affect the loss of CCI and canopy greenness of our beech  
460 saplings, their mortality, and the onset of the loss of canopy greenness in our mature trees. The effect of  
461 the drought stress on the loss of canopy greenness might be due to an early leaf abscission in response to  
462 hydraulic failure of the branches (Wolfe et al., 2016; Munné-Bosch and Alegre, 2004). For the mature trees,  
463 the different drought response of the autumn pattern of chlorophyll (no effect) and the loss of canopy  
464 greenness (advanced and enhanced) is probably an important reason of confusion still present today in  
465 the literature on the relationship between drought and autumn senescence.

466  
467 The continuously computed rainfall deficit was similar between 2018 and 2019. Nevertheless, the loss of  
468 canopy greenness suggests that the drought of 2019, which coincided with several heat waves, might have  
469 been less damaging for the late-summer leaf dynamics than the drought of 2018. The rainfall deficit



470 starting from a zero deficit supports the observation that, despite the accumulated drought effect, the  
471 drought of 2019 was less severe in the growing season than the drought of 2018. Perhaps, the conditions  
472 of 2018 (i.e. sunny and warm with high vapor pressure deficits) triggered the damaging process of  
473 cavitation in the trees, while this might have occurred less intensively in 2019 if the stomatal conductance  
474 was lower (Barigah et al., 2013; Bolte et al., 2016; Banks et al., 2019). Alternatively, the difference in the  
475 timing of the drought peaks (i.e. the drought of 2018 peaked slightly earlier than the drought of 2019)  
476 could have led to divergent responses due to differences in drought sensitivity along the growing season  
477 (Banks et al., 2019).

478  
479 The drought stress did not affect the onset of autumn leaf senescence of both the beech saplings and the  
480 mature trees. Deciduous trees therefore seem to have a conservative strategy concerning the timing of  
481 their autumn leaf senescence that might be under the control of a constant variable (e.g. the day-length  
482 or photo spectrum) (Michelson et al., 2018; Chiang et al., 2019). Such a strategy prioritizes carbon uptake  
483 over nutrient remobilization, as a fixed onset of autumn leaf senescence would not allow an advanced  
484 nutrient remobilization when required (Keskitalo et al., 2005; Brelford et al., 2019). Moreover, such a  
485 strategy makes the trees vulnerable against the effects of early frost. In case of early frost, the trees might  
486 not complete their nutrient resorption. Possible consequences of an incomplete nutrient resorption over  
487 a longer time period might include a decline in the overall fitness of the trees and negative feedbacks on  
488 the growth dynamics of the next season, such as less buds (Fu et al., 2014; Vander Mijnsbrugge et al.,  
489 2016; Crabbe et al., 2016).

490  
491 Surprisingly, the onset of autumn leaf senescence did not differ significantly among the different tree  
492 species, which supports the idea that the onset of autumn leaf senescence in different deciduous trees  
493 might be controlled by the same (light related) signal. Other explanations for this result could be the small  
494 sample size (i.e. 8 beech, 4 birch and 4 oak trees for the CCI) or the inaccuracies related to the method of  
495 piece-wise linear regressions. Given our results, the drought in 2018 and 2019 had little impact on the CCI  
496 trend and onset of autumn leaf senescence in mature beech, birch and oak trees.

497  
498 Although the onset of autumn leaf senescence in both the tree saplings and the mature trees was not  
499 advanced by drought stress, the onset of autumn leaf senescence in beech saplings was around 22 days  
500 earlier than mature beech trees. Such difference could be due to the different growing conditions (pots  
501 versus normal soil), environmental conditions at the different sites, the difference in the average leaf age  
502 (tree saplings have an earlier bud-burst than mature trees) or the different ecophysiological response of  
503 tree saplings and mature trees (e.g. tree saplings are more vulnerable than mature trees and therefore  
504 are likely to use different functional strategies) (Niinemets, 2010; Vander Mijnsbrugge et al., 2016; Pšidová  
505 et al., 2015). As there is very little difference in the light conditions among the different sites, the  
506 difference in the day length is unlikely to have affected the difference in the timing of the onset of autumn  
507 leaf senescence between the beech saplings and mature trees. However, it is possible that the beech  
508 saplings have a different sensitivity to the light cues, as they usually grow in the understory and therefore  
509 under a different light regime than mature trees (Brelford et al., 2019; Michelson et al., 2018; Chiang et  
510 al., 2019).

511  
512 Concerning the onset of the loss of canopy greenness for all species and opposed to 2017 (i.e. a year with  
513 normal environmental conditions in late-summer and autumn) and 2019 (i.e. a year with high  
514 temperatures in summer, relatively normal precipitation in summer and autumn, but suffering from the  
515 accumulated effects of the rainfall deficit), the onset of the loss of canopy greenness in 2018 was around  
516 three-and-a-half weeks earlier. The canopy greenness metric had been declining earlier in 2018 because  
517 the leaves have likely shed earlier due to an advanced leaf abscission process to protect the tree from



518 hydraulic failure (Munné-Bosch and Alegre, 2004; Wolfe et al., 2016). There was also a difference in the  
519 onset of the loss of canopy greenness among the species. This might be due to two reasons. First, birch  
520 (the species with the earliest onset of the loss of canopy greenness) has an indeterministic growth pattern,  
521 which also means continuous leaf mortality. Second, the fact that oak (the species with the latest onset  
522 of the loss of canopy greenness) has typically a second leaf flush, which might connect the difference  
523 between beech and oak to differences in leaf longevity.

## 524 5. Conclusion

525 The different environmental conditions of three years (comprising a severe dry year and a severe warm  
526 year) did not affect the timing of the onset of autumn leaf senescence in mature beech, birch and oak  
527 forest trees in Belgium. This suggests that deciduous trees have a conservative strategy concerning the  
528 timing of their senescence. Like our mature beech trees, beech saplings exposed to a drought also did not  
529 show any advancement in their onset of autumn leaf senescence compared to beech saplings in normal  
530 conditions. Although the drought stress did not affect the timing of the onset of autumn leaf senescence,  
531 it is clear from our results that the drought stress did affect the mortality rate in tree saplings and the leaf  
532 mortality in mature trees.

## 533 6. Acknowledgements

534 The authors acknowledge the funding provided by the ERC Starting Grant LEAF-FALL (714916) and the  
535 DOCPRO4 fellowship provided to BM by the University of Antwerp. We also express our gratitude to the  
536 Flemish Institute for Nature and Forest (INBO), the Integrated Carbon Observation System (ICOS), the  
537 Belgian Royal Meteorological Institute (KMI) and the Royal Dutch Meteorological Institute (KNMI) for  
538 providing meteorological data. We would also thank the Agency for Forest and Nature of the Flemish  
539 Government (ANB), the Belgian Armed Forces and the Municipality of Brasschaat because they gave  
540 permission to conduct research in the study areas. Special thanks are due to Dirk Leyssens (ANB) and  
541 Bergen boomverzorging.

## 542 7. Author contributions

543 MC and HDB designed the experiment. ID, SL, PW and BM collected the data. PW computed the rainfall  
544 deficit, while BM performed all other analyses. BM, PW and MC wrote the text. All authors contributed to  
545 the discussions.

## 546 8. References

- 547 Banks, J. M., Percival, G. C., and Rose, G.: Variations in seasonal drought tolerance rankings, *Trees*, 33,  
548 1063-1072, 10.1007/s00468-019-01842-5, 2019.
- 549 Barigah, T. S., Charrier, O., Douris, M., Bonhomme, M., Herbette, S., Ameglio, T., Fichot, R., Brignolas, F.,  
550 and Cochard, H.: Water stress-induced xylem hydraulic failure is a causal factor of tree mortality in  
551 beech and poplar, *Ann. Bot.*, 112, 1431-1437, 10.1093/aob/mct204, 2013.
- 552 Bates, D., Mächler, M., Bolker, B., and Walker, S.: Fitting Linear Mixed-Effects Models Using lme4, *Journal*  
553 *of Statistical Software*, 67, 1-48, 10.18637/jss.v067.i01, 2015.
- 554 Benbella, M., and Paulsen, G. M.: Efficacy of Treatments for Delaying Senescence of Wheat Leaves: II.  
555 Senescence and Grain Yield under Field Conditions, *Agron. J.*, 90, 332-338,  
556 10.2134/agronj1998.00021962009000030004x, 1998.
- 557 Bolte, A., Czajkowski, T., Coccozza, C., Tognetti, R., de Miguel, M., Psidova, E., Ditmarova, L., Dinca, L.,  
558 Delzon, S., Cochard, H., Raebild, A., de Luis, M., Cvjetkovic, B., Heiri, C., and Muller, J.: Desiccation and



- 559 Mortality Dynamics in Seedlings of Different European Beech (*Fagus sylvatica* L.) Populations under  
560 Extreme Drought Conditions, *Front Plant Sci*, 7, 751, 10.3389/fpls.2016.00751, 2016.
- 561 Brelford, C. C., Trasser, M., Paris, T., Hartikainen, S. M., and Robson, T. M.: Understory light quality  
562 affects leaf pigments and leaf phenology in different plant functional types, *bioRxiv*, 829036,  
563 10.1101/829036, 2019.
- 564 Brunner, I., Herzog, C., Dawes, M. A., Arend, M., and Sperisen, C.: How tree roots respond to drought,  
565 *Front Plant Sci*, 6, 547, 10.3389/fpls.2015.00547, 2015.
- 566 Buck, A. L.: New Equations for Computing Vapor Pressure and Enhancement Factor, *Journal of Applied*  
567 *Meteorology*, 20, 1527-1532, 10.1175/1520-0450(1981)020<1527:Nefcvp>2.0.Co;2, 1981.
- 568 Bultot, F., Coppens, A., and Dupriez, G. L.: Estimation de l'évapotranspiration potentielle en Belgique :  
569 (procédure révisée), Bruxelles : Institut royal météorologique de Belgique, 1983.
- 570 Campioli, M., Verbeeck, H., Van den Bossche, J., Wu, J., Ibrom, A., D'Andrea, E., Matteucci, G., Samson,  
571 R., Steppe, K., and Granier, A.: Can decision rules simulate carbon allocation for years with contrasting  
572 and extreme weather conditions? A case study for three temperate beech forests, *Ecol. Model.*, 263, 42-  
573 55, 10.1016/j.ecolmodel.2013.04.012, 2013.
- 574 Chiang, C., Olsen, J. E., Basler, D., Bankstad, D., and Hoch, G.: Latitude and Weather Influences on Sun  
575 Light Quality and the Relationship to Tree Growth, *Forests*, 10, 610, ARTN 610  
576 10.3390/f10080610, 2019.
- 577 Crabbe, R. A., Dash, J., Rodriguez-Galiano, V. F., Janous, D., Pavelka, M., and Marek, M. V.: Extreme  
578 warm temperatures alter forest phenology and productivity in Europe, *Sci Total Environ*, 563-564, 486-  
579 495, 10.1016/j.scitotenv.2016.04.124, 2016.
- 580 De Boeck, H. J., and Verbeeck, H.: Drought-associated changes in climate and their relevance for  
581 ecosystem experiments and models, *Biogeosciences*, 8, 1121-1130, 10.5194/bg-8-1121-2011, 2011.
- 582 De Boeck, H. J., De Groote, T., and Nijs, I.: Leaf temperatures in glasshouses and open-top chambers,  
583 *New Phytol*, 194, 1155-1164, 10.1111/j.1469-8137.2012.04117.x, 2012.
- 584 Estiarte, M., and Penuelas, J.: Alteration of the phenology of leaf senescence and fall in winter deciduous  
585 species by climate change: effects on nutrient proficiency, *Glob. Chang. Biol.*, 21, 1005-1017,  
586 10.1111/gcb.12804, 2015.
- 587 Fox, J., and Weisberg, S.: *An {R} Companion to Applied Regression*, Third ed., Sage, Thousand Oaks (CA),  
588 2019.
- 589 Fracheboud, Y., Luquez, V., Bjorken, L., Sjodin, A., Tuominen, H., and Jansson, S.: The control of autumn  
590 senescence in European aspen, *Plant Physiol.*, 149, 1982-1991, 10.1104/pp.108.133249, 2009.
- 591 Fu, Y., Campioli, M., Vitasse, Y., De Boeck, H., Berge, J., Abdelgawad, H., Asard, H., Piao, S., Deckmyn, G.,  
592 and Janssens, I.: Variation in leaf flushing date influences autumnal senescence and next year's flushing  
593 date in two temperate tree species, *Proc Natl Acad Sci U S A*, 111, 10.1073/pnas.1321727111, 2014.
- 594 Gallinat, A. S., Primack, R. B., and Wagner, D. L.: Autumn, the neglected season in climate change  
595 research, *Trends Ecol Evol*, 30, 169-176, 10.1016/j.tree.2015.01.004, 2015.
- 596 Gárate-Escamilla, H., Brelford, C. C., Hampe, A., Robson, T. M., and Garzón, M. B.: Greater capacity to  
597 exploit warming temperatures in northern populations of European beech is partly driven by delayed  
598 leaf senescence, *Agricultural and Forest Meteorology*, 284, 107908, 10.1016/j.agrformet.2020.107908,  
599 2020.
- 600 Garnier, S.: *viridis: Default Color Maps from 'matplotlib'*. 2018.
- 601 Gill, A. L., Gallinat, A. S., Sanders-DeMott, R., Rigden, A. J., Short Gianotti, D. J., Mantooth, J. A., and  
602 Templer, P. H.: Changes in autumn senescence in northern hemisphere deciduous trees: a meta-analysis  
603 of autumn phenology studies, *Ann. Bot.*, 116, 875-888, 10.1093/aob/mcv055, 2015.
- 604 Hastie, T., and Tibshirani, R.: *Generalized Additive Models*, *Statistical Science*, 1, 297-310, 1986.



- 605 Holm, G.: Chlorophyll Mutations in Barley, *Acta Agric Scand*, 4, 457-471, 10.1080/00015125409439955,  
606 1954.
- 607 Hörtensteiner, S., and Feller, U.: Nitrogen metabolism and remobilization during senescence, *J. Exp.*  
608 *Bot.*, 53, 927-937, 10.1093/jexbot/53.370.927, 2002.
- 609 Hothorn, T., Bretz, F., and Westfall, P.: Simultaneous Inference in General Parametric Models, *Biom J*,  
610 50, 346-363, 2008.
- 611 IPCC: Climate change 2014: synthesis report. Contribution of Working Groups I, II and III to the fifth  
612 assessment report of the Intergovernmental Panel on Climate Change. Core Writing Team, R. K. P. a. L.  
613 A. M. e. (Ed.), IPCC, Geneva, Switzerland, 2014.
- 614 Kassambara, A.: ggpubr: 'ggplot2' Based Publication Ready Plots. 2019.
- 615 Keskitalo, J., Bergquist, G., Gardestrom, P., and Jansson, S.: A cellular timetable of autumn senescence,  
616 *Plant Physiol.*, 139, 1635-1648, 10.1104/pp.105.066845, 2005.
- 617 KMI: Klimatologisch sezoenoverzicht, lente 2017, 2017a.
- 618 KMI: Klimatologisch sezoenoverzicht, zomer 2017, 2017b.
- 619 KMI: Klimatologisch sezoenoverzicht, herfst 2017, 2017c.
- 620 KMI: Klimatologisch sezoenoverzicht, zomer 2018, 2018a.
- 621 KMI: Klimatologisch sezoenoverzicht, herfst 2018, 2018b.
- 622 KMI: Klimatologisch sezoenoverzicht, herfst 2019, 2019a.
- 623 KMI: Klimatologisch sezoenoverzicht, zomer 2019, 2019b.
- 624 Koike, T.: Autumn coloring, photosynthetic performance and leaf development of deciduous broad-  
625 leaved trees in relation to forest succession, *Tree Physiology*, 7, 21-32, 10.1093/treephys/7.1-2-3-4.21,  
626 1990.
- 627 Leul, M., and Zhou, W.: Alleviation of waterlogging damage in winter rape by application of uniconazole:  
628 Effects on morphological characteristics, hormones and photosynthesis, *Field Crops Res.*, 59, 121-127,  
629 [https://doi.org/10.1016/S0378-4290\(98\)00112-9](https://doi.org/10.1016/S0378-4290(98)00112-9), 1998.
- 630 Leuzinger, S., Zotz, G., Asshoff, R., and Korner, C.: Responses of deciduous forest trees to severe drought  
631 in Central Europe, *Tree Physiol*, 25, 641-650, 10.1093/treephys/25.6.641, 2005.
- 632 Mariën, B., Balzarolo, M., Dox, I., Leys, S., Lorene, M. J., Geron, C., Portillo-Estrada, M., AbdElgawad, H.,  
633 Asard, H., and Campioli, M.: Detecting the onset of autumn leaf senescence in deciduous forest trees of  
634 the temperate zone, *New Phytol*, 224, 166-176, 10.1111/nph.15991, 2019.
- 635 Matile, P.: Biochemistry of Indian summer: physiology of autumnal leaf coloration, *Exp Gerontol*, 35,  
636 145-158, [https://doi.org/10.1016/S0531-5565\(00\)00081-4](https://doi.org/10.1016/S0531-5565(00)00081-4), 2000.
- 637 Medawar, P. B.: *The Uniqueness of the individual*, by P.B. Medawar, Methuen, London, 1957.
- 638 Menzel, A., Helm, R., and Zang, C.: Patterns of late spring frost leaf damage and recovery in a European  
639 beech (*Fagus sylvatica* L.) stand in south-eastern Germany based on repeated digital photographs, *Front*  
640 *Plant Sci*, 6, 110, 10.3389/fpls.2015.00110, 2015.
- 641 Michelson, I. H., Ingvarsson, P. K., Robinson, K. M., Edlund, E., Eriksson, M. E., Nilsson, O., and Jansson,  
642 S.: Autumn senescence in aspen is not triggered by day length, *Physiol Plant*, 162, 123-134,  
643 10.1111/ppl.12593, 2018.
- 644 Munné-Bosch, S., and Alegre, L.: Die and let live: leaf senescence contributes to plant survival under  
645 drought stress, *Funct. Plant Biol.*, 31, 10.1071/fp03236, 2004.
- 646 Niinemets, Ü.: Responses of forest trees to single and multiple environmental stresses from seedlings to  
647 mature plants: Past stress history, stress interactions, tolerance and acclimation, *For. Ecol. Manage.*,  
648 260, 1623-1639, 10.1016/j.foreco.2010.07.054, 2010.
- 649 Novick, K. A., Ficklin, D. L., Stoy, P. C., Williams, C. A., Bohrer, G., Oishi, A. C., Papuga, S. A., Blanken, P.  
650 D., Noormets, A., Sulman, B. N., Scott, R. L., Wang, L. X., and Phillips, R. P.: The increasing importance of  
651 atmospheric demand for ecosystem water and carbon fluxes, *Nature Climate Change*, 6, 1023-1027,  
652 10.1038/Nclimate3114, 2016.





- 653 Pedersen, E. J., Miller, D. L., Simpson, G. L., and Ross, N.: Hierarchical generalized additive models in  
654 ecology: an introduction with mgcv, *PeerJ*, 7, e6876, 10.7717/peerj.6876, 2019.
- 655 Penman, H. L.: Natural evaporation from open water, bare soil and grass, *Proc R Soc Lond A Math Phys*  
656 *Sci*, 193, 120-145, 10.1098/rspa.1948.0037, 1948.
- 657 Pšidová, E., Ditmarová, L., Jamnická, G., Kurjak, D., Majerová, J., Czajkowski, T., and Bolte, A.:  
658 Photosynthetic response of beech seedlings of different origin to water deficit, *Photosynthetica*, 53,  
659 187-194, 10.1007/s11099-015-0101-x, 2015.
- 660 R Core Team: R: A language and environment for statistical computing. R Foundation for Statistical  
661 Computing, Vienna, Austria, 2020.
- 662 Richardson, A. D., Keenan, T. F., Migliavacca, M., Ryu, Y., Sonnentag, O., and Toomey, M.: Climate  
663 change, phenology, and phenological control of vegetation feedbacks to the climate system, *Agricultural*  
664 *and Forest Meteorology*, 169, 156-173, 10.1016/j.agrformet.2012.09.012, 2013.
- 665 Rigby, R. A., and Stasinopoulos, D. M.: Generalized additive models for location, scale and shape, *Journal*  
666 *of the Royal Statistical Society Series C-Applied Statistics*, 54, 507-544, DOI 10.1111/j.1467-  
667 9876.2005.00510.x, 2005.
- 668 Seyednasrollah, B., Young, A. M., Li, X., Milliman, T., Ault, T., Froking, S., Friedl, M., and Richardson, A.  
669 D.: Sensitivity of Deciduous Forest Phenology to Environmental Drivers: Implications for Climate Change  
670 Impacts Across North America, *Geophys. Res. Lett.*, 47, e2019GL086788, 10.1029/2019gl086788, 2020.
- 671 Simpson, G. L.: gratia: Graceful 'ggplot'-Based Graphics and Other Functions for GAMs Fitted Using  
672 'mgcv'. 2020.
- 673 Turcsan, A., Steppe, K., Sarkozi, E., Erdelyi, E., Missoorten, M., Mees, G., and Mijnsbrugge, K. V.: Early  
674 Summer Drought Stress During the First Growing Year Stimulates Extra Shoot Growth in Oak Seedlings  
675 (*Quercus petraea*), *Front Plant Sci*, 7, 193, 10.3389/fpls.2016.00193, 2016.
- 676 Van den Berge, J., Naudts, K., Zavalloni, C., Janssens, I. A., Ceulemans, R., and Nijs, I.: Altered response to  
677 nitrogen supply of mixed grassland communities in a future climate: a controlled environment  
678 microcosm study, *Plant Soil*, 345, 375-385, 10.1007/s11104-011-0789-8, 2011.
- 679 van der Werf, G. W., Sass-Klaassen, U. G. W., and Mohren, G. M. J.: The impact of the 2003 summer  
680 drought on the intra-annual growth pattern of beech (*Fagus sylvatica* L.) and oak (*Quercus robur* L.) on a  
681 dry site in the Netherlands, *Dendrochronologia*, 25, 103-112, 10.1016/j.dendro.2007.03.004, 2007.
- 682 Vander Mijnsbrugge, K., Turcsan, A., Maes, J., Duchene, N., Meeus, S., Steppe, K., and Steenackers, M.:  
683 Repeated Summer Drought and Re-watering during the First Growing Year of Oak (*Quercus petraea*)  
684 Delay Autumn Senescence and Bud Burst in the Following Spring, *Front Plant Sci*, 7, 419,  
685 10.3389/fpls.2016.00419, 2016.
- 686 Vitasse, Y., François, C., Delpierre, N., Dufrêne, E., Kremer, A., Chuine, I., and Delzon, S.: Assessing the  
687 effects of climate change on the phenology of European temperate trees, *Agricultural and Forest*  
688 *Meteorology*, 151, 969-980, 10.1016/j.agrformet.2011.03.003, 2011.
- 689 Vito, M., and Muggeo, R.: segmented: an R Package to Fit Regression Models with Broken-Line  
690 Relationships, *R News*, 8, 20-25, 2008.
- 691 Vonwettstein, D.: Chlorophyll-letale und der submikroskopische Formwechsel der Plastiden, *Exp. Cell*  
692 *Res.*, 12, 427-506, 10.1016/0014-4827(57)90165-9, 1957.
- 693 Wang, S., Yang, B., Yang, Q., Lu, L., Wang, X., and Peng, Y.: Temporal Trends and Spatial Variability of  
694 Vegetation Phenology over the Northern Hemisphere during 1982-2012, *PLoS ONE*, 11, e0157134,  
695 10.1371/journal.pone.0157134, 2016.
- 696 Wickham, H.: ggplot2: Elegant Graphics for Data Analysis, Springer-Verlag, New York, 2009.
- 697 Wickham, H., Francois, R., Henry, L., and Müller, K.: dplyr: A Grammar of Data Manipulation. 2018.
- 698 Wilke, C. O.: cowplot: Streamlined Plot Theme and Plot Annotations for 'ggplot2'. 2019.



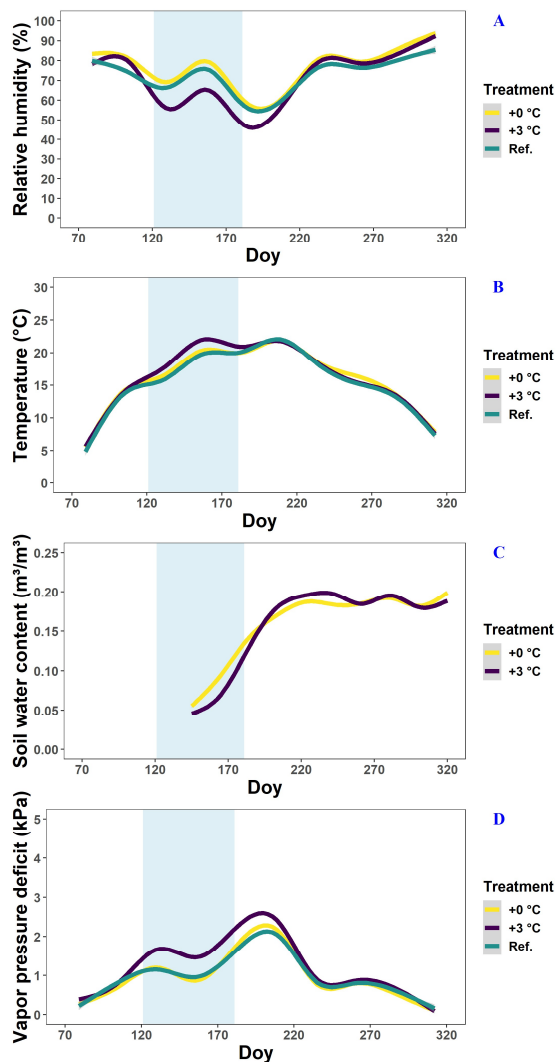


699 Willems, P.: Compound intensity/duration/frequency-relationships of extreme precipitation for two  
700 seasons and two storm types, *Journal of Hydrology*, 233, 189-205, 10.1016/S0022-1694(00)00233-x,  
701 2000.  
702 Willems, P.: Multidecadal oscillatory behaviour of rainfall extremes in Europe, *Clim. Change*, 120, 931-  
703 944, 10.1007/s10584-013-0837-x, 2013.  
704 Wolfe, B. T., Sperry, J. S., and Kursar, T. A.: Does leaf shedding protect stems from cavitation during  
705 seasonal droughts? A test of the hydraulic fuse hypothesis, *New Phytol*, 212, 1007-1018,  
706 10.1111/nph.14087, 2016.  
707 Wood, S. N.: Fast stable restricted maximum likelihood and marginal likelihood estimation of  
708 semiparametric generalized linear models, *J. Roy. Stat. Soc. Ser. B. (Stat. Method.)*, 73, 3-36,  
709 10.1111/j.1467-9868.2010.00749.x, 2011.  
710 Xie, Y., and Wilson, A. M.: Change point estimation of deciduous forest land surface phenology, *Remote*  
711 *Sens. Environ.*, 240, 111698, 10.1016/j.rse.2020.111698, 2020.  
712 Zeileis, A., and Hothorn, T.: Diagnostic Checking in Regression Relationships, *R News*, 2, 7-10, 2002.  
713 Zeng, H., Jia, G., and Epstein, H.: Recent changes in phenology over the northern high latitudes detected  
714 from multi-satellite data, *Environmental Research Letters*, 6, 045508, 10.1088/1748-9326/6/4/045508,  
715 2011.  
716 Zuur, A., Ieno, E., and Smith, G.: *Analysing Ecological Data*, *Statistics for Biology and Health*, 2007.  
717 Zuur, A. F., Ieno, E. N., and Elphick, C. S.: A protocol for data exploration to avoid common statistical  
718 problems, *Methods Ecol. Evol.*, 1, 3-14, 10.1111/j.2041-210X.2009.00001.x, 2010.  
719 Zuur, A. F., Ieno, E. N., and Freckleton, R.: A protocol for conducting and presenting results of regression-  
720 type analyses, *Methods Ecol. Evol.*, 7, 636-645, 10.1111/2041-210x.12577, 2016.

721

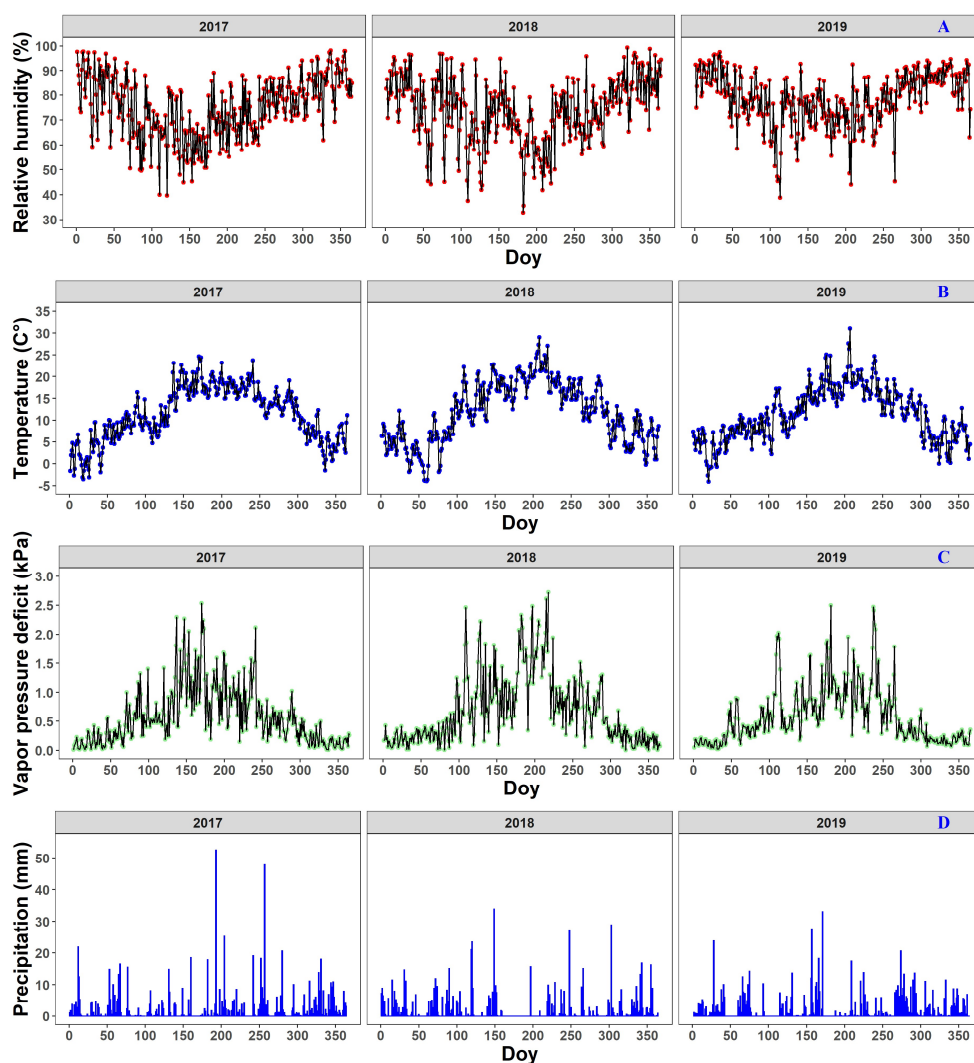


722 Figures

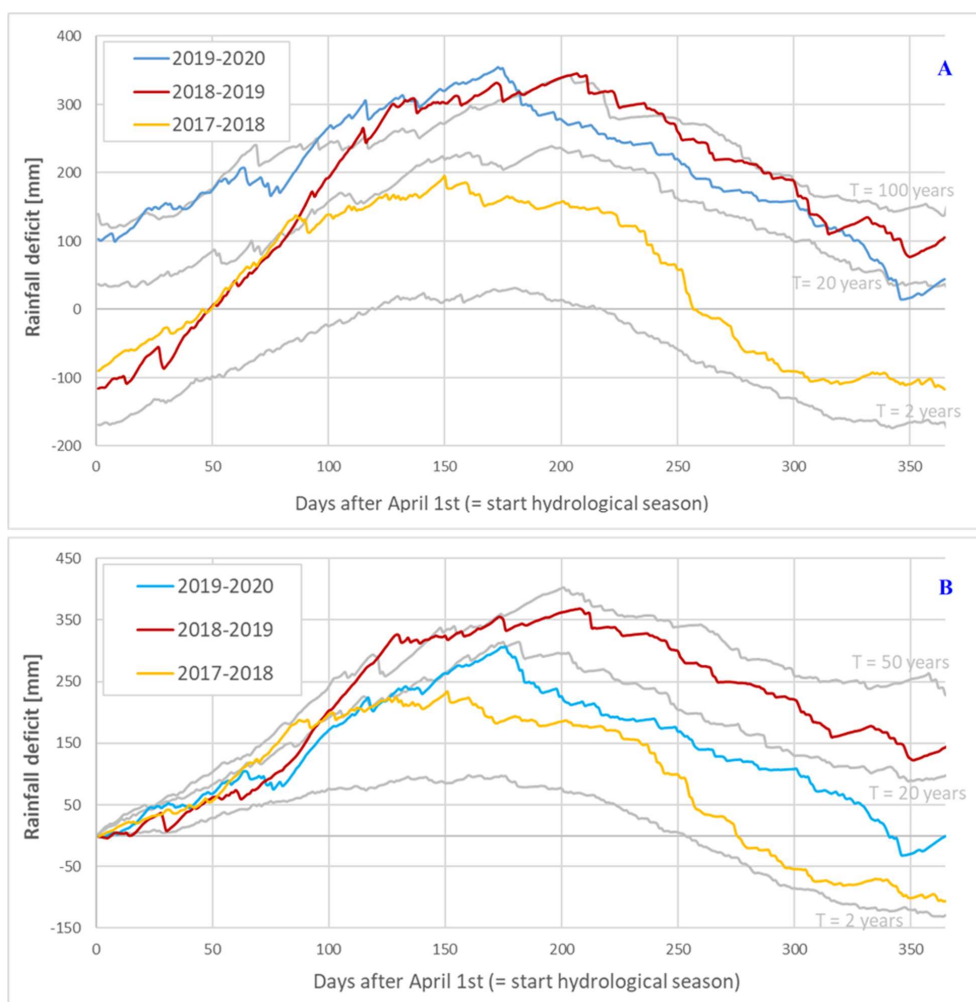


723

724 Fig. 1: The relative humidity (panel A), temperature (panel B), soil water content (panel C) and  
725 vapor pressure deficit (panel D) in the glasshouses and outside plots at the Drie Eiken Campus in Wilrijk. Solid  
726 lines represent regressions of half-hourly measurements of the relative humidity (%), temperature (°C),  
727 and soil water content (m<sup>3</sup>/m<sup>3</sup>). The vapor pressure deficit (kPa) was calculated using the formulas of Buck  
728 (1981) using data of the relative humidity and air temperature between 7 a.m. and 7 p.m. Green, blue and  
729 red lines represent the conditions in the reference plots (Ref.), glasshouses that follow the outside  
730 ambient air temperature (+0 °C) and glasshouses that are three degrees warmer than the outside  
731 ambient air temperature (+3 °C), respectively. The light blue band represents the treatment-period.



732  
733 Fig. 2: The meteorological conditions near the Klein Schietveld and Park of Brasschaat. The line plots  
734 represent the daily average relative humidity (%; red), temperature (°C; blue) and vapor pressure deficit  
735 (kPa; green), while the bar plots represent the daily precipitation (mm; light blue). The data was measured  
736 every half hour and provided by the Flemish Institute for Nature and Forest (INBO), the Integrated Carbon  
737 Observation System (ICOS) and the Royal Dutch Meteorological Institute (KNMI). The vapor pressure deficit (kPa)  
738 was calculated using the formulas of Buck (1981) using data of the relative humidity and air  
739 temperature between 7 a.m. and 7 p.m.  
740  
741



742

743 Fig. 3: The rainfall deficit for the meteorological station of the Royal Meteorological Institute (KMI) in  
744 Ukkel, Belgium. The colored solid lines represent the rainfall deficit for the hydrological years in the period  
745 2017-2020, while the grey solid lines represent the long-term reference statistics (computed for the 100-  
746 year period 1901 - 2000) with T as the return period, which represents the mean time between two  
747 successive exceedances of a given deficit value and is computed in an empirical way (Willem, 2000, 2013).  
748 Panel A uses a continuous computation, while panel B starts from a zero deficit on the first of April (the  
749 start of the hydrological year). The colors represent the rainfall deficit in 2017 (light blue), 2018 (red) and  
750 2019 (yellow).  
751

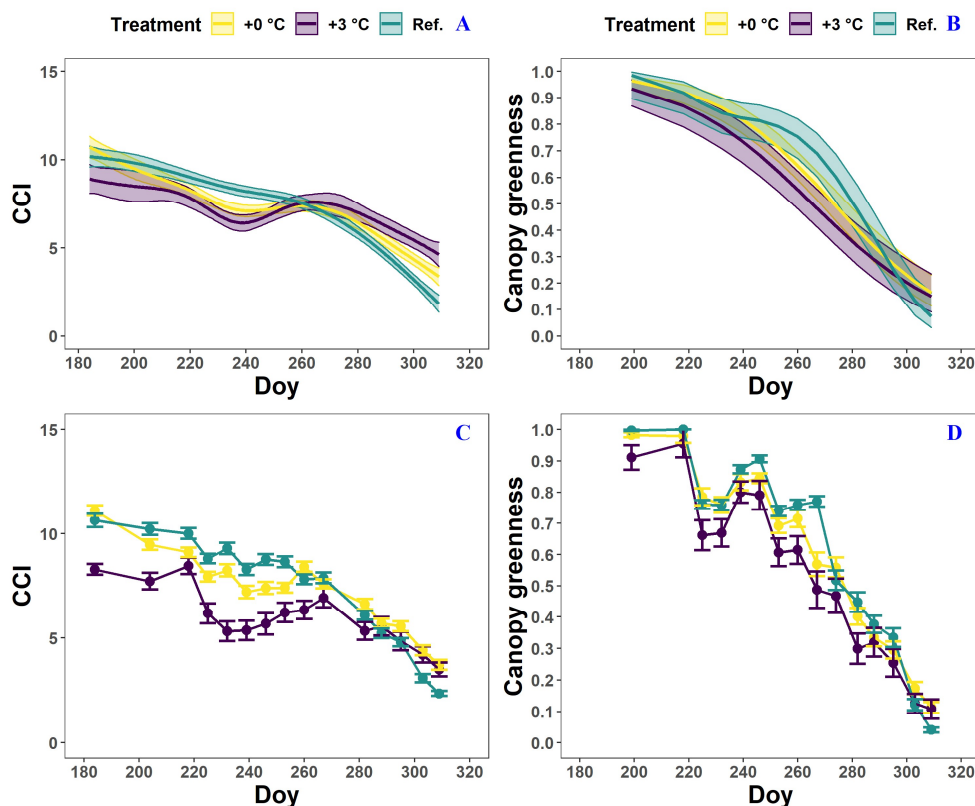
751

752



753

754



755

756

757

758

759

760

761

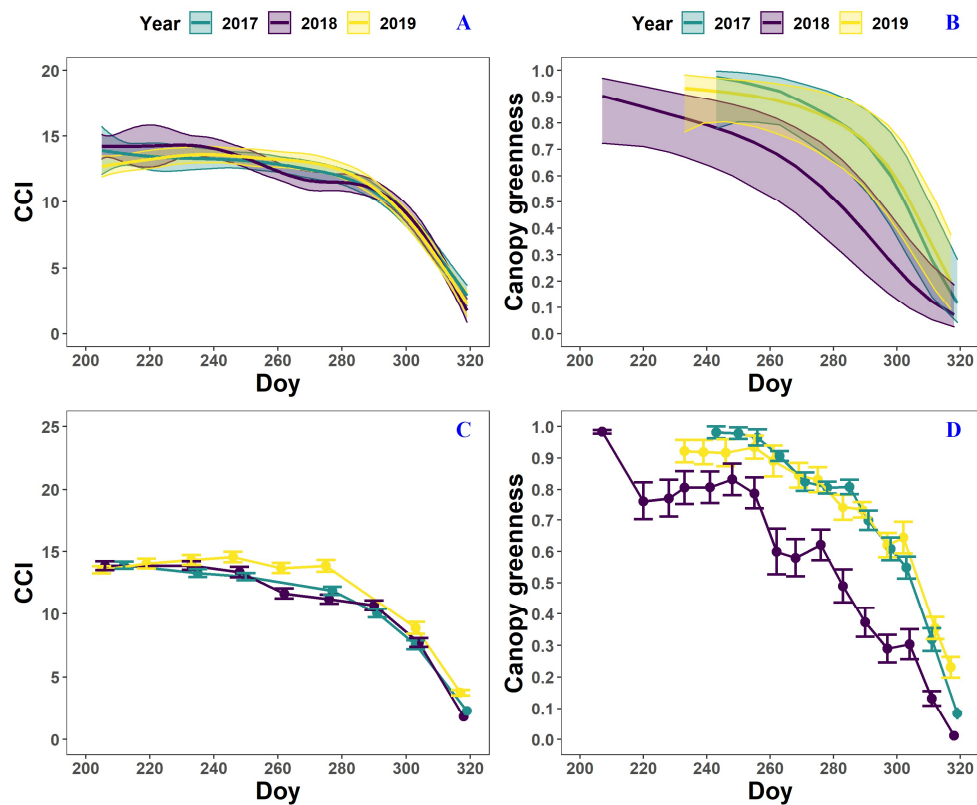
762

763

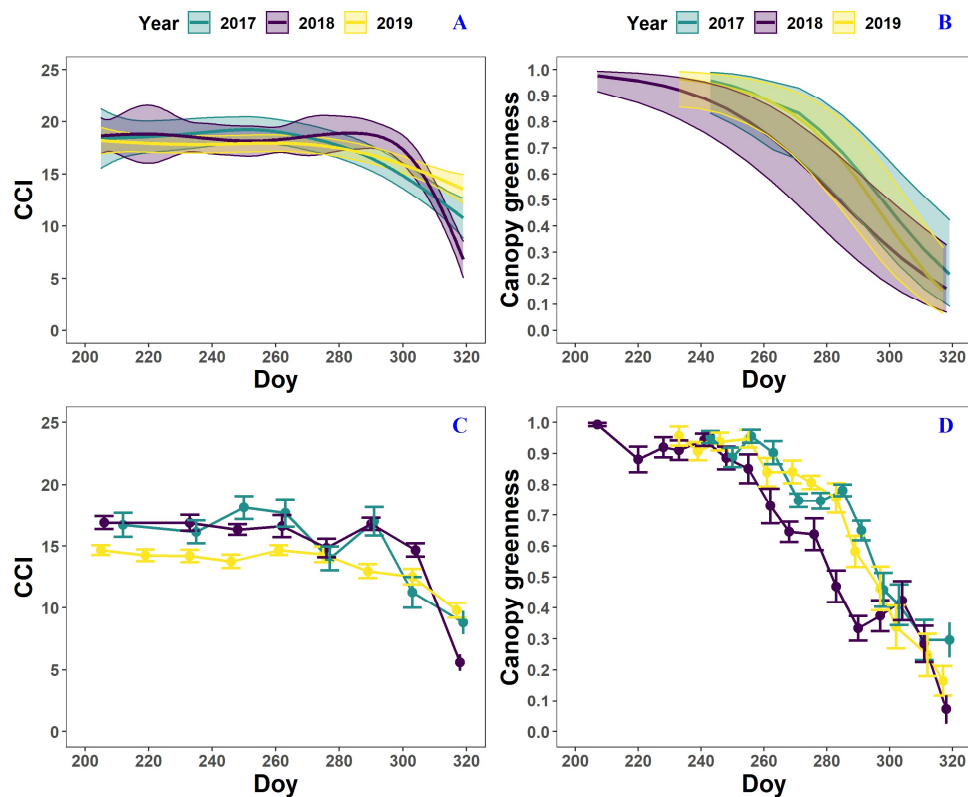
764

765

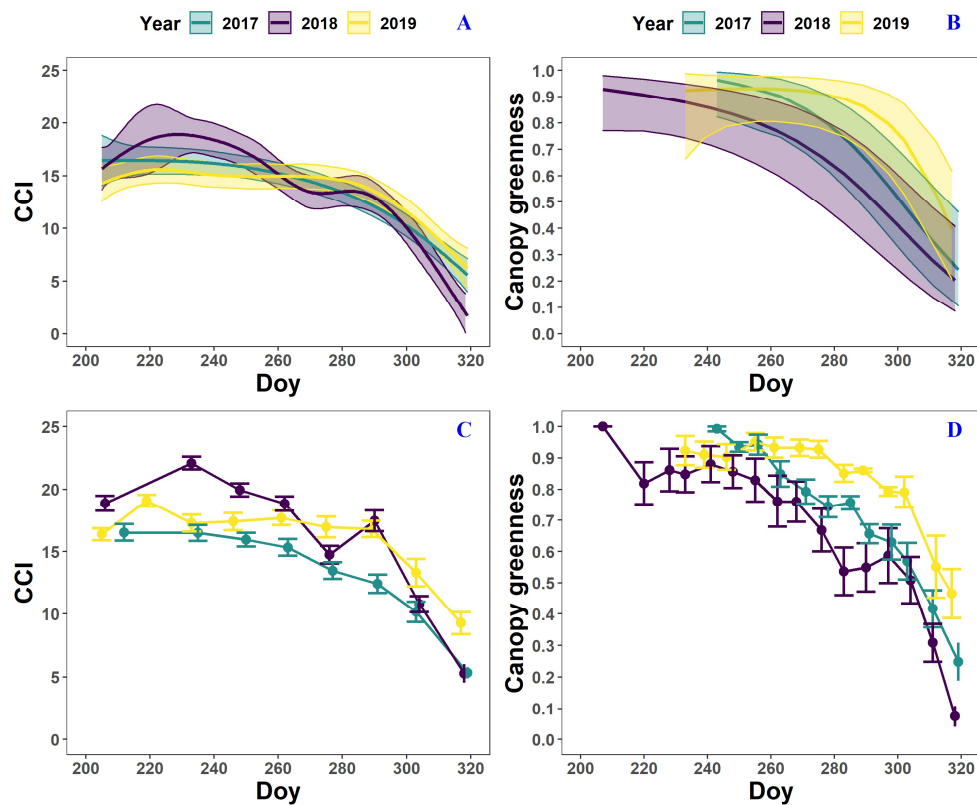
Fig. 4: The generalized additive mixed model fits for the chlorophyll content index (CCI; panel A) and loss of canopy greenness (panel B) of the *Fagus sylvatica* saplings at the Drie Eiken Campus in Wilrijk. The colored solid lines represent smooth terms, while the colored shaded bands around the smooth terms represent approximate 95% simultaneous confidence intervals (panel A) and 95% pointwise confidence intervals (panel B). The dots and error bars represent the mean CCI (panel C) and mean canopy greenness (panel D) with standard errors. The colors represent the CCI or the loss of canopy greenness of the beech saplings in the reference plots (green; Ref.), the glasshouses that followed the outside ambient air temperature (yellow; +0 °C) and the glasshouses that were three degrees warmer than the outside ambient air temperature (purple; +3 °C), respectively.



766  
767 Fig. 5: The generalized additive mixed model fits for the chlorophyll content index (CCI;  $n = 8$ ; panel A) and  
768 loss of canopy greenness ( $n = 16$ ; panel B) of the mature *Fagus sylvatica* trees at the Klein Schietveld and  
769 Park of Brasschaat. The colored solid lines represent smooth terms, while the colored shaded bands  
770 around the smooth terms represent approximate 95% simultaneous confidence intervals (panel A) and  
771 95% pointwise confidence intervals (panel B). The dots and error bars represent the mean CCI (panel C)  
772 and mean canopy greenness (panel D) with standard errors. The colors represent the CCI or the loss of  
773 canopy greenness of the mature beech trees in 2017 (green), 2018 (purple) and 2019 (yellow).  
774



775  
776 Fig. 6: The generalized additive mixed model fits for the chlorophyll content index (CCI;  $n = 4$ ; panel A) and  
777 loss of canopy greenness ( $n = 8$ ; panel B) of the mature *Betula pendula* trees at the Klein Schietveld. The  
778 colored solid lines represent smooth terms, while the colored shaded bands around the smooth terms  
779 represent approximate 95% simultaneous confidence intervals (panel A) and 95 % pointwise confidence  
780 intervals (panel B). The dots and error bars represent the mean CCI (panel C) and mean canopy greenness  
781 (panel D) with standard errors. The colors represent the CCI or the loss of canopy greenness of the mature  
782 birch trees in 2017 (green), 2018 (purple) and 2019 (yellow).  
783



784  
785 Fig. 7: The generalized additive mixed model fits for the chlorophyll content index (CCI;  $n = 4$ ; panel A) and  
786 loss of canopy greenness ( $n = 8$ ; panel B) of the mature *Quercus robur* trees at the Klein Schietveld. The  
787 colored solid lines represent smooth terms, while the colored shaded bands around the smooth terms  
788 represent approximate 95% simultaneous confidence intervals (panel A) and 95% pointwise confidence  
789 intervals (panel B). The dots and error bars represent the mean CCI (panel C) and mean canopy greenness  
790 (panel D) with standard errors. The colors represent the CCI or the loss of canopy greenness of the mature  
791 oak trees in 2017 (green), 2018 (purple) and 2019 (yellow).  
792





793 **Tables**

794 **Table 1:** Overview of the meteorological conditions perceived by the mature trees in the Klein Schietveld  
 795 and Park of Brasschaat. All data is measured by the meteorological station of the Royal Meteorological  
 796 Institute (KMI) in Ukkel, Belgium (KMI, 2018b, a, 2017c, b, 2019a, b). The degree of abnormality of the  
 797 values is represented by (a; abnormal values that happen on average once every 6 years) and (e;  
 798 exceptional values that happen on average once every thirty years). Since 2019, the KMI uses a new  
 799 system to show the degree of abnormality. Values that are with the five highest values since 1981 are  
 800 marked by (+), while values within the three highest values are marked by (++)  
 801

	Normal (1981-2010)		2017		2018		2019	
	summer	autumn	summer	autumn	summer	autumn	summer	autumn
<b>Average temperature (°C)</b>	17.6	10.9	18.6 (a)	11.3	19.8 (e)	11.8	19.1 (++)	11.3
<b>Total precipitation (mm)</b>	224.6	219.9	179.9	226.5	134.7 (a)	168.5	198.6	209.3
<b>Average number of rainy days</b>	43.9	51	44	63 (a)	20 (e)	32 (e)	33	53
<b>Relative humidity (%)</b>	73	82	67.7 (e, June)	62	62.3 (e, July)	75 (e, July)	70	83
<b>Sunshine duration (h:m)</b>	578:20	322:00	573:21	322:00	693:06 (a)	471:12 (e)	714:38 (++)	322:23
<b>Global solar radiation (kWh/m<sup>2</sup>)</b>	429.6	168.2	447.1 (a, June)	233.8	498.6 (e, July)	213.4 (e, October)	487.9 (+)	178.4

802  
 803



804 Table 2: Adjusted  $R^2$ , effective degrees of freedom (edf) and F-test values of the GAMM smooth terms. All  
 805 smooth terms were significant, with p-values < 0.001.  $\mathbb{E}(y_i)$  are the expected values of the response  
 806 variable  $y_i$ ,  $f(x_i)$  is the smooth function of the covariate  $x_i$ ,  $\beta_i$  is the intercept of the covariate  $x_i$ ,  $\zeta$  is the  
 807 random effect and  $\epsilon_i$  are the errors. All smooth functions were fitted using P-splines. The chlorophyll  
 808 content index, loss of canopy greenness, day of the year and tree individual are abbreviated by CCI, LOCG,  
 809 Doy and ID, respectively.  
 810

Site	Species	$Y_i$	Model equation	Family distribution	Link function	Adjusted $R^2$	Smooth term	Treatment	Edf	F or Chi.sq
Wilrijk	<i>Fagus sylvatica</i>	CCI	(1) $g(\mathbb{E}(y_i)) = f_1 \text{Treatment}_i(\text{Doy}_i) + \beta_1 \text{Treatment}_i + \beta_2 \text{Leaf\_place}_i + \zeta_{ID} + \epsilon_i$	Gaussian	Identity	0.61	Day of the year	Reference	4.8	337.5
								+0 °C	5.8	175
								+3 °C	6.1	34.4
Wilrijk	<i>Fagus sylvatica</i>	Loss of canopy greenness	(2) $g(\mathbb{E}(y_i)) = f_1 \text{Treatment}_i(\text{Doy}_i) + \beta_1 \text{Treatment}_i + \zeta_{ID} + \epsilon_i$	Binomial	Logit	0.76	Day of the year	Reference	3.6	112.6
								+0 °C	1.1	105.9
								+3 °C	1	53.7
Year										
KS & PB	<i>Fagus sylvatica</i>	CCI	(3) $g(\mathbb{E}(y_i)) = f_1 \text{Year}_i(\text{Doy}_i) + \beta_1 \text{Year}_i + \beta_2 \text{Leaf\_type}_i + \zeta_{ID} + \epsilon_i$	Gaussian	Identity	0.7	Day of the year	2017	4.6	197.8
								2018	5.3	221.6
								2019	5.2	193.2
KS & PB	<i>Fagus sylvatica</i>	Loss of canopy greenness	(4) $g(\mathbb{E}(y_i)) = f_1 \text{Year}_i(\text{Doy}_i) + \beta_1 \text{Year}_i + \zeta_{ID} + \epsilon_i$	Binomial	Logit	0.87	Day of the year	2017	2.4	44.8
								2018	2.5	70.6
								2019	2.7	66
KS	<i>Betula pendula</i>	CCI	(5) $g(\mathbb{E}(y_i)) = f_1 \text{Year}_i(\text{Doy}_i) + \beta_1 \text{Year}_i + \beta_2 \text{Leaf\_type}_i + \zeta_{ID} + \epsilon_i$	Gaussian	Identity	0.44	Day of the year	2017	3.2	25.9
								2018	5	56.9
								2019	3.1	14.7
KS	<i>Betula pendula</i>	Loss of canopy greenness	(6) $g(\mathbb{E}(y_i)) = f_1 \text{Year}_i(\text{Doy}_i) + \beta_1 \text{Year}_i + \zeta_{ID} + \epsilon_i$	Binomial	Logit	0.89	Day of the year	2017	1	20.6
								2018	1	36
								2019	1.6	48.2
PB	<i>Quercus robur</i>	CCI	(7) $g(\mathbb{E}(y_i)) = f_1 \text{Year}_i(\text{Doy}_i) + \beta_1 \text{Year}_i + \beta_2 \text{Leaf\_type}_i + \zeta_{ID} + \epsilon_i$	Gaussian	Identity	0.52	Day of the year	2017	3.3	62.5
								2018	5.1	84.4
								2019	4.3	30.7
PB	<i>Quercus robur</i>	Loss of canopy greenness	(8) $g(\mathbb{E}(y_i)) = f_1 \text{Year}_i(\text{Doy}_i) + \beta_1 \text{Year}_i + \zeta_{ID} + \epsilon_i$	Binomial	Logit	0.85	Day of the year	2017	1.2	12.5
								2018	1.9	33.6
								2019	2.4	32

811